ACADEMIC
PRESS

A simple scheme for the design of solvent-suppression pulses

Élise Prost,[a] Philippe Sizun,[b] Martial Piotto,[c] and Jean-Marc Nuzillard[a],*

[a] *Pharmacognosy Laboratory, UMR-A 6013 CNRS, CPCBAI, Bat. 18, BP 1039, Moulin de la Housse, 51687 Reims Cedex 2, France*
[b] *Sanofi-Synthélabo Recherche, 371 rue du Pr. Blayac, 34184, Montpellier Cedex 4, France*
[c] *Application Laboratory, Bruker France, 34 rue de l'Industrie, 67166 Wissembourg, France*

Abstract

Excitation sculpting was first introduced as a way to efficiently suppress solvent signals. It requires a pulse sequence that acts as a null pulse at the solvent-resonance frequency and as an inversion pulse everywhere else. In this article, it is shown that such a goal can be achieved starting with "top-hat" inversion shaped pulses such as I-BURP-2 or gaussian cascade G3. The result is a Globally Antisymmetric Selective Pulse, or GASP. Numerical optimization was used to extend the performance of such pulses. Multifrequency signal suppression was shown to be possible through application of successive excitation sculpting modules.
© 2002 Elsevier Science (USA). All rights reserved.

Keywords: Solvent suppression; Excitation sculpting; BURP

1. Introduction

Solvent-suppression techniques in NMR were initially applied to the study of biological molecules dissolved in undeuterated water. LC–NMR coupling rapidly developed when efficient solvent-suppression schemes became available, thus avoiding the use of highly expensive deuterated solvents as the chromatographic medium. More recently, the need for productivity enhancement and cost control in industry led to the design of new automated analytical systems. Such an approach relies on LC–NMR hardware to eliminate the cost of NMR sample tubes and deuterated solvents. The creation of such a system in one of our laboratories (P.S.) incited us to carry out an evaluation of the presently used solvent-peak-suppression techniques and to investigate new possibilities.

The most widely used solvent-signal-suppression techniques for LC–NMR are solvent presaturation [1] and WET techniques [2]. This is due to their strong insensitivity to experimental conditions, as well as their use in multiple solvent situations. The suppression bandwidth is also very narrow and signals close to those of the solvent(s) can still be observed. The WATERGATE scheme [3] opened the way to other gradient-enhanced spin echo techniques [4,5] that provide an extremely high level of solvent signal rejection; we therefore focused our attention on this class of experiments.

The underlying theory [4] is briefly reported below.

2. Principle

2.1. Excitation sculpting

Any pulse and delay sequence S, applied to a non-coupled spin collection characterized by its offset frequency Ω, can be described by a rotation in the physical three-dimensional space. The orientation of the rotation axis is defined by the two polar angles $\theta(\Omega)$ and $\phi(\Omega)$. This rotation transforms the equilibrium magnetization vector $(0, 0, M_0)$ into a vector $(M_{xz}(\Omega), M_{yz}(\Omega), M_{zz}(\Omega))$, both expressed in the rotating frame of reference. The inversion probability $P(\Omega)$ is defined as

$$P(\Omega) = \frac{1 - M_{zz}/M_0}{2}. \tag{1}$$

*Corresponding author. Fax: +33-3-26-91-35-96.
E-mail addresses: elise.prost@univ-reims.fr (É. Prost), philippe.sizun@sanofi-synthelabo.fr (P. Sizun), martial.piotto@bruker.fr (M. Piotto), jm.nuzillard@univ-reims.fr (J.-M. Nuzillard).

The gradient echo sequence G–S–G rotates the *transverse* component of the magnetization vector by an angle $2\phi(\Omega)$ around the OZ axis and scales it by the $P(\Omega)$ factor, itself being defined from the transformation of the initial *longitudinal* equilibrium state. The $2\phi(\Omega)$ rotation introduces an unwanted offset-dependent phase variation. Conversely, the double echo pulse sequence G_1–S–G_1–G_2–S–G_2, designed for "excitation sculpting," only scales the transverse magnetization by the factor $P^2(\Omega)$ and does not introduce any phase alteration, providing that gradient pulses G_1 and G_2 have different intensities or directions. The pulse sequence made of a hard $\pi/2$ pulse followed by a double echo has thus an excitation profile identical to the square of the inversion probability profile of sequence S.

In order to apply this very general result to a solvent-peak-suppression scheme, a sequence S needs to be found which ideally achieves $P(\Omega = 0) = 0$ and $P(\Omega \neq 0) = 1$. After a non-selective excitation pulse, the double echo sequence will preserve the magnetization of all nuclei but those at $\Omega = 0$, a natural place for the solvents giving rise to only one spectral peak. Obviously, transverse relaxation during the whole echo time leads to non-negligible signal loss, especially if large fast relaxing macromolecules are studied. However, the situation is less critical for small molecules of synthetic or biological origin submitted to automated routine analysis.

2.2. Zero degree pulses

The success of the gradient echo technique strongly relies on the condition $P(0) = 0$. An ideal inversion probability profile would be that in Fig. 1a, where the width of the non-inversion zone should be as narrow as possible. However, it is more physically realistic to obtain a profile like the one in Fig. 1b.
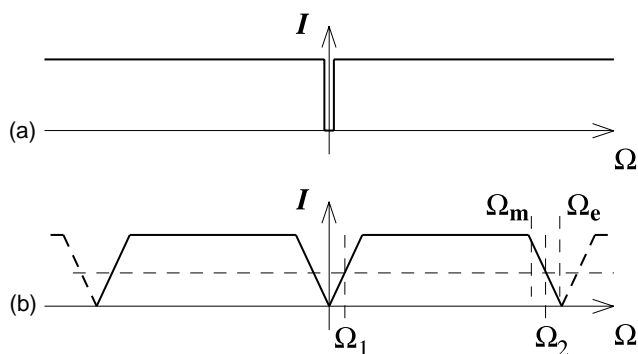

Fig. 1. Theoretical excitation profiles for a single solvent-signal-suppression. Intensity I as a function of offset Ω is the relative amount of transverse magnetization that is preserved by the solvent-suppression sequence. (a) Ideal profile. (b) Realistic profile. The offsets Ω_1 and Ω_2 correspond to the first crossing through the 50% intensity line, and to the second crossing point, respectively. The wide dotted lines suggest the profile of pseudo-periodic sequences like the one based on W5.

The offset Ω_1 is half the width of the peak suppression hole. Clearly, there will always be an offset Ω_2 so that for any $\Omega > \Omega_2$, the inversion efficiency will decrease due to offset effect. The ratio $M = \Omega_2/\Omega_1$ represents an interesting figure of merit that defines the width of the "hole" by comparison to the overall usable excitation bandwidth. The ratio should be as high as possible because once a minimal value of Ω_1 is chosen as an acceptable higher limit, the excitation band-width to be covered must be as wide as possible.

The condition $P(0) = 0$ forces the sequence S to globally behave as a zero degree pulse for on-resonance nuclei. A way to achieve this goal is to use a fully anti-symmetric sequence: $B_1(t) = -B_1(T - t)$, where B_1 is the complex excitation field $B_{1x} + iB_{1y}$ and T the sequence length. Under this condition the flip angle at $\Omega = 0$ is

$$\gamma \left| \int_0^T B_1(t)\, dt \right| = 0. \tag{2}$$

The greatest advantage of this approach lies in its insensitivity to B_1 miscalibration and inhomogeneities [4]. Multiplying B_1 by any factor in Eq. (2) will leave the latter unchanged.

The sequence $3\alpha_x$–τ–$9\alpha_x$–τ–$19\alpha_x$–τ–$19\alpha_{-x}$–τ–$9\alpha_{-x}$–τ–$3\alpha_{-x}$ with $26\alpha = \pi$ known as "3-9-19" [6] has a 0 and π flip angle for $\Omega = 0$ and $\Omega = 1/2\tau$, respectively. It presents a $1/\tau$ period and a figure of merit $M = 5.2$ ($\gamma B_1/2\pi = 25\,\text{kHz}$). The figure of merit can be improved by extending the concept to 8 and 10 hard pulses, resulting in the W4 and W5 sequences [7], for which the individual pulse angles were determined by numerical optimization. A value of $M = 8.9$ was obtained for W5.

Higher values of M can be expected by developing $B_1(t)$ over an appropriate set of analytic basis functions and to optimize the parameters to fit the obtained inversion profile with the ideal one. Instead of directly following this not so straightforward route we first decided to use the "tools of the trade" and to adapt them to solvent-peak-suppression. The basic idea is to have the first part of the pulse $(0 \leqslant t \leqslant T)$ refocusing the magnetization of the nuclei with $\Omega < 0$ and the second part $(T \leqslant t \leqslant 2T)$ acting on those with $\Omega > 0$. Let $B_1^0(t)$ be the shape (hereafter named the source shape) of an inversion pulse for which $M_{zz}(\Omega)$ is an even function, and whose duration is T. The pulse whose length is $2T$ and that is defined as

$$B_1(t) = B_1^0(t)e^{-i\Omega_S t} \quad 0 \leqslant t \leqslant T,$$
$$B_1(t) = B_1^0(2T - t)e^{-i\Omega_S(2T - t)} \quad T \leqslant t \leqslant 2T \tag{3}$$

is antisymmetrical because $B_1(t) + B_1(2T - t) = 0$. It thus achieves a zero degree flip angle at $\Omega = 0$. Such a pulse is a Globally Antisymmetric Selective Pulse, or GASP. Its first part is simply the source shape to which a frequency shift Ω_S is applied [8]. The shift is chosen so that the falling edge of the inversion profile is close to

$\Omega = 0$. The second part of the pulse is deduced from the first one by time-inversion (t becomes $T - t$), time translation ($T - t$ becomes $2T - t$) and amplitude inversion. The time-reversal operation changes the frequency shift from Ω_S to $-\Omega_S$, as desired. The whole process is illustrated in Fig. 2, in which the source shape is an optimized version of I-BURP-2 (*vide infra*). The result may be seen as a kind of 180° Janus pulse [9], built like a Jump–Return sequence [10]. Once the source shape is chosen, the only parameter that must be adjusted is Ω_S, or better, the dimensionless value of $\epsilon = \Omega_S T / 2\pi$. Time (and signal) could be gained by replacing the GASP pulse of length $2T$ by one of length T defined by

$$B_1(t) = B_1^0(t)\mathrm{e}^{-\mathrm{i}\Omega_S t} - B_1^0(T - t)\mathrm{e}^{-\mathrm{i}\Omega_S(T-t)}, \quad (4)$$

which is also antisymmetrical. Indeed, this would be correct if there were a linear relationship between the excitation field and the response profile. The non-linear behavior of the physical system leads to useless inversion profiles, in such a way that was already analyzed in the context of "close encounters between soft pulses" [11].

Many radiofrequency modulation shapes are eligible for band-selective spin inversion. It is necessary to keep the GASP length as short as possible for a given value of Ω_2, which is of the order of magnitude of the width $2\pi\Delta\nu$ of the inversion profile generated by $B_1^0(t)$. A high value of M can be reached if the width of the transition zone between inversion and non-inversion is small, relative to the inversion band-width. Adiabatic inversion pulses [12] seemed to be good candidates as source shapes, as they are able to cover a wide frequency range within a small time interval. However, their rather wide transition zone would lead to using unacceptably high B_1 fields to obtain Ω_1 values compatible with the observation of sample signals close to the solvent resonance line.

Inversion pulses I-BURP-2 [13] and G3 [14] were then considered as source shapes, due to their "top-hat" inversion probability profile. The maximum of M as a function of ϵ is located at $\epsilon = 2.63$ with $M = 13.9$ for I-BURP-2 and $\epsilon = 2.35$ with $M = 10.6$ for G3. These M values are significantly higher than those obtained for the

W5 pulse ($M = 8.9$). The calculations were carried out using home-written software. The action of each element of the selective pulse is calculated as the result of a rotation around the effective tilted field in the rotating frame of reference.

2.3. Pulse shape optimization

The optimization of the source shape for its incorporation in a GASP pulse was then investigated. The I-BURP-2 pulse was chosen as the starting point because it showed a slightly higher M value than G3. A BURP pulse is defined by $B_1(t)$ so that

$$\frac{\gamma B_1(t)}{2\pi}T = 0.5 + \sum_{k=1}^{n} A_k \cos\left(\frac{2\pi kt}{T}\right) + B_k \sin\left(\frac{2\pi kt}{T}\right), \quad (5)$$

where n is the order of this Fourier expansion, and A_k and B_k its coefficients. The term 0.5 ensures that the overall flip angle is π. The published value of n for I-BURP-2 is 11 and was augmented to 13; the supplementary A_k and B_k parameters were set to 0. The knowledge of an acceptable initial set of parameter values led us to consider optimization through the simplex algorithm [15].

For a GASP of 2 ms duration, obtained from I-BURP-2 ($T = 1$ ms), the extended excitation bandwidth $2\Omega_e/2\pi$ (see Fig. 1) was imposed to be 14 kHz and the minimum excitation bandwidth to be $2\Omega_m/2\pi = 12$ kHz. This target was reached and led to $\Omega_1/2\pi = 322$ Hz, $\Omega_2/2\pi = 6500$ Hz, and therefore to a figure of merit $M = 20.2$. The frequency shift $\Omega_S/2\pi$ was found to be equal to 3329 Hz.

The parameters of the corresponding I-BURP shape are listed in Table 1. As usual, all frequencies, including
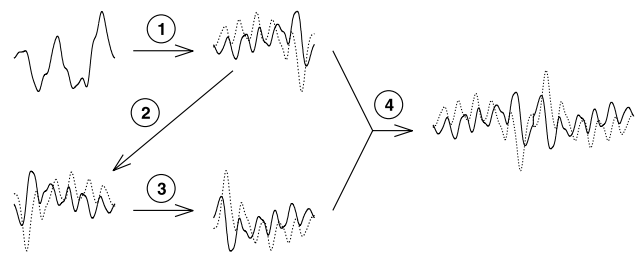

Fig. 2. Construction of a Globally Antisymmetric Selective Pulse. The initial RF profile is frequency-shifted (step 1) to build the first part of the GASP. The latter is time-reversed (step 2), intensity-reversed (step 3) and the result joined to the end of the first part (step 4). Solid and dashed lines represent the real and imaginary parts of the RF profiles, respectively.

Table 1
This table gives the A_k and B_k coefficients for the optimized I-BURP-2 pulse that is used for the construction of a GASP pulse

k	A_k	B_k
0	0.5	–
1	1.158095	−0.547503
2	0.831757	−1.621601
3	−0.864658	0.655359
4	−0.811595	−0.020694
5	−0.105315	0.349345
6	−0.013964	−0.117996
7	0.087210	−0.021530
8	−0.043993	0.270062
9	0.161185	−0.096931
10	−0.015727	−0.068322
11	−0.103811	−0.017366
12	−0.111983	0.091530
13	0.066988	−0.048717

The corresponding value of ϵ is 3.329. For calibration purposes, the radiofrequency attenuation that must be applied relative to a rectangular pulse of identical duration is 19.8 dB.

the excitation "hole" width and the frequency shift are inversely proportional to pulse length.

Despite the promising performance of the optimized GASP pulse, it lacks the independence of ϕ from the offset presented by W5. Attempting to use a GASP pulse in a single echo experiment requires a complex phase correction process. Its parameters are derived from the numerical simulation of the GASP pulse action. This phase correction causes strong base-line distorsion and requires a robust base-line correction algorithm [16], thus making GASP pulses difficult to use in simple echo sequences.

Surprisingly, computation also showed that a 10% misset of the radio-frequency field strength does not have a significant impact on the intensity of the sample response in its nominal frequency range. The bad reputation of BURP pulses relative to their intolerance to miscalibration are not justified in this context.

2.4. Multiple solvent suppression

The problem that was then studied dealt with the suppression of two solvent signals. In presaturation and WET techniques, a simple sine modulation of the selective radio-frequency field creates two side-bands that can be moved to the desired offsets [17]. A more recent approach uses excitation sculpting but relies on the correct calibration of hard and soft inversion pulses [18]. A simple analysis shows that this method fails when directly transposed to the double gradient echo scheme. A simple work around solution was found. It consisted of applying two successive double echo sequences, each of them being frequency shifted to the offset of a solvent-resonance frequency. The resulting excitation profile is simply the product of the individual profiles, as described in Fig. 4a. For a $\Delta\Omega$ shift, the useful excitation bandwidth $2\Omega_2$ is reduced to $2\Omega_2 - 2\Delta\Omega$. The need for high values of M is clearly justified in the context of multiple suppression. Multiplication by a factor of 2 of the delay between excitation and detection may seem unrealistic for biological molecules, but it may still prove useful for small molecule analysis.

3. Results

A comparison of the experimental excitation profiles derived from W5, I-BURP-2, and GASP-optimized I-BURP-2 are presented in Fig. 3. The employed sequences contained four gradient pulses (1 ms each) and two zero degree pulses (2 ms each), resulting in an overall 8 ms delay between initial sample excitation and signal acquisition.

The measured M values 9.6, 12.3, and 20.9 are close to those obtained by numerical simulation. For GASP-optimized I-BURP-2, we showed that for the test sample containing a 1 mM sucrose solution in 90% H_2O–10%
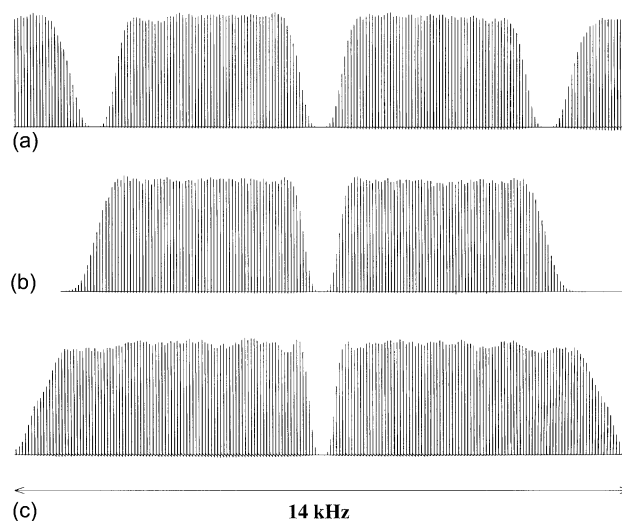

Fig. 3. Experimental excitation profiles for solvent-suppression pulses embedded in $\pi/2$-double echo sequences with identical overall duration (8 ms). The sample is $CuSO_4$-doped water ($T_2 \approx 500$ ms) in D_2O. Each spectrum is acquired by means of a single scan. The offsets vary from −7000 to +7000 Hz in 70 Hz steps. The zero degree pulses are (a) W5, (b) GASP from I-BURP-2, (c) GASP from optimized I-BURP-2.

D_2O, the anomeric proton at 5.32 ppm was left untouched by the water signal suppression. The spectrum obtained by presaturation of the water signal was taken as reference. Attenuation of 66% and 45% of the anomeric signal was observed with W5 and unoptimized GASP from I-BURP-2, with an identical overall length of the suppression pulse sequence.

The excitation profile in Fig. 4b was obtained by means of two successive double echoes, thus showing the possibility of suppression of two solvent signals. The spectra corresponding to exact inversions of the solvent signal (in the ellipses) are magnified to show that peak residue intensity falls close to the noise level. This high attenuation level makes it possible to deal with highly diluted samples in the context of LC–NMR coupling.

The spectrum in Fig. 4c is that of 1 mM sucrose in water(W)–acetonitrile(ACN), a typical binary HPLC solvent system. The four echoes may be either paired (echo(W)–echo(W)–echo(ACN)–echo(ACN)) or interleaved (echo(W)–echo(ACN)–echo(ACN)–echo(W)) within the pulse sequence. The latter possibility gave rise to a slightly better suppression level, but no attempt was made to interpret this observation. The presence of four echoes has a noticeable effect on multiplet patterns. The observed phase distorsion is due to the action of homonuclear couplings on transverse magnetization during τ_e, the total echo time: 8 ms for a single solvent, and 16 ms for the spectrum in Fig. 4c. The outermost components of a multiplet of width W present a $\pi W \tau_e$ phase error. Therefore, the widest multiplets are the most affected, and the phase distorsion observed in Fig. 4c is reduced to half in single solvent-resonance-suppression spectra.
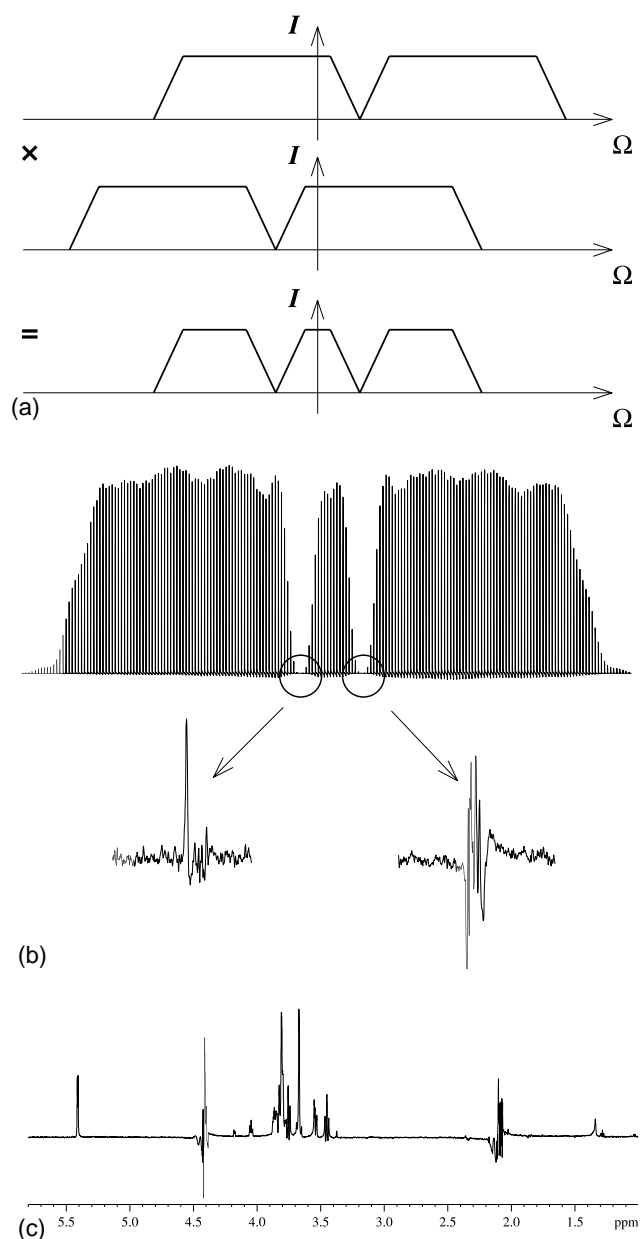
Fig. 4. (a) Prediction of the overall excitation profile (lower trace) for two successive double echoes applied at two different offsets (upper traces). (b) The corresponding experimental profile, recorded in the same conditions as in Fig. 3. In the first double echo, the soft pulses are shifted by +700 Hz, and by −700 Hz in the second double echo. (c) The spectrum of 1 mM of sucrose in a mixture of acetonitrile (45%), water (45%), and D_2O (10%). Eight transients were recorded, with heteronuclear decoupling during acquisition to remove the ^{13}C satellites of acetonitrile.

4. Conclusion

Solvent-signal suppression is cleanly achieved through the double inversion sequences designed by Shaka and Canet. The key element in their pulse sequences is obtaining a true zero degree pulse for on-resonance nuclei, independent of B_1 miscalibration or inhomogeneity. In this article we present a simple way of deriving new zero degree pulses from previously described inversion "top-hat" pulses. They benefit from the design that ensures a low sensitivity to experimental conditions and a minimal pulse calibration procedure. The pulse derived from I-BURP-2 may be used as a starting point for further enhancement through numerical optimization. The resulting shaped pulse is not optimal but its practical use provides the expected quality of solvent suppression. It has also been shown that the concatenation of frequency shifted double echoes can be used for multiple solvent suppression, but the application is mainly limited to the study of small molecules dissolved in non-deuteriated solvents.

References

[1] D.I. Hoult, Solvent peak saturation with single phase and quadrature Fourier transformation, J. Magn. Reson. 21 (1976) 337–347.

[2] S.H. Smallcombe, S.L. Patt, P.A. Keifer, WET solvent suppression and its application to LC NMR and high-resolution NMR spectroscopy, J. Magn. Reson. A 117 (1995) 295–303.

[3] M. Piotto, V. Saudek, V. Sklenář, Gradient tailored excitation for single quantum spectroscopy of aqueous solutions, J. Biomol. NMR 2 (1992) 661–665.

[4] T.-L. Hwang, A.J. Shaka, Water suppression that works. Excitation sculpting using arbitrary waveforms and pulses field gradients, J. Magn. Reson. A 112 (1995) 275–279.

[5] C. Roumestand, D. Canet, Extending the excitation sculpting concept for selective excitation, J. Magn. Reson. 147 (2000) 275–279.

[6] V. Sklenář, M. Piotto, R. Leppik, V. Saudek, Gradient-tailored water suppression for ^1H–^{15}N HSQC experiments optimized to retain full sensitivity, J. Magn. Reson. A 102 (1993) 241–245.

[7] M. Liu, X. Mao, C. Ye, H. Huang, J.K. Nicholson, J.C. Lindon, Improved WATERGATE Pulse sequences for solvent suppression in NMR spectroscopy, J. Magn. Reson. 132 (1998) 125–129.

[8] S.L. Patt, Single- and multiple-frequency-shifted laminar pulses, J. Magn. Reson. 96 (1992) 94–102.

[9] Ē. Kupče, R. Freeman, Pulse design in the frequency domain, J. Magn. Reson. A 103 (1993) 358–363.

[10] P. Plateau, M. Guéron, Exchangeable proton NMR without baseline distortion, using new strong-pulse sequences, J. Am. Chem. Soc. 104 (1982) 7310–7311.

[11] Ē. Kupče, R. Freeman, Close encounters between soft pulses, J. Magn. Reson. A 112 (1995) 261–264.

[12] Ē. Kupče, R. Freeman, Adiabatic pulses for wideband inversion and broadband decoupling, J. Magn. Reson. A 115 (1995) 273–276.

[13] H. Geen, R. Freeman, Band-selective radiofrequency pulses, J. Magn. Reson. 93 (1991) 93–141.

[14] L. Emsley, G. Bodenhausen, Gaussian pulse cascades, new analytical functions for rectangular selective inversion and

in-phase excitation in NMR, Chem. Phys. Lett. 165 (1990) 469–476.

[15] W.H. Press, S.A. Teutolsky, W.T. Vetterling, B.P. Flannery, Numerical Recipes in C, second ed., Cambridge University Press, New York, NY, 1992.

[16] J.-L. Pons, T.E. Malliavin, M.-A. Delsuc, Gifa V. 4: a complete package for NMR data set processing, J. Biomol. NMR 8 (1996) 445–452.

[17] R. Konrat, I. Burghardt, G. Bodenhausen, Coherence transfer in nuclear magnetic resonance by selective homonuclear Hartmann–Hahn correlation spectroscopy, J. Am. Chem. Soc. 113 (1991) 9135–9140.

[18] C. Dalvit, G. Shapiro, J.-M. Böhlen, T. Parella, Technical aspects of an efficient multiple solvent-suppression technique, Magn. Reson. Chem. 37 (1999) 7–14.